TASK QUARTERLY 9 No 4, 439–448

USABILITY OF SELECTED TURBULENCE MODELS FOR SIMULATION FLOW THROUGH A PIPE ORIFICE

BOLESŁAW DOBROWOLSKI, KRZYSZTOF KRĘCISZ AND ANDRZEJ SPYRA

Chair of Thermal Engineering and Industrial Facilities,
Faculty of Mechanical Engineering, Technical University of Opole,
Mikołajczyka 5, 45-271 Opole, Poland
{bolo, aspr}@po.opole.pl

(Received 31 January 2005; revised manuscript received 15 September 2005)

Abstract: A modern CFD code was used to simulate fluid flow through a pipeline with an orifice. A two-dimensional flow was assumed. The influence of the turbulence model and the size of the numerical grid on the quality of the obtained results was tested. It appears from the performed calculations that the standard Launder-Spalding k-ε model yields the best results for two-dimensional flows through pipeline-orifice systems.

Keywords: CFD, turbulence models, orifice, flow simulation

1. Introduction

For over thirty years now, a new trend has been developing in the research of fluid and gas flows, which uses computer simulation of flows based on the Navier-Stokes or Reynolds equations. At present, computers make it possible to simulate even very complicated phenomena. The cost of a computer simulation is usually much lower than that of an equivalent experiment. Moreover, computer simulation offers complete data on the quantities characterizing the simulated flow, while in an experiment such data can only be obtained with specialized and very expensive apparatuses [1].

When computer simulations of a flow through a pipeline with an orifice are concerned, we often wonder, whether the simulation produces a precise image of the real flow. The question is not answered easily, as the quality of the obtained results depends on many parameters of the computer model (see Erdal and Anderson [2], Hilgenstock and Ernst [3]). Spencer *et al.* [4] have reported that even simulations of the same flow with use of the same program can produce different results when they are realized by other research teams. Modern CFD programs offer their users many possible parameters of the mathematical model. However, if various turbulence models are available, the user may wonder which of them is the best suited for a pipeline-orifice system. The authors attempt to answer this question in the present paper.

2. Mathematical model

Let us consider two-dimensional flow of a viscous incompressible fluid through a straight segment of a pipeline with an orifice. The considered system is shown in Figure 1 (page 444). The fluid motion is described by a set of equations called the Reynolds-averaged Navier-Stokes (RANS) equations, containing the equations of motion:

$$\rho\mathbf{U}\nabla\cdot\mathbf{U} = -\nabla p + \nabla\mu_{\text{ef}}\cdot(\nabla\mathbf{U} + \nabla\mathbf{U}^T) + \frac{2}{3}\rho\nabla k \tag{1}$$

and equations of continuity:

$$\nabla\cdot\mathbf{U} = 0, \tag{2}$$

where $\mathbf{U}$ is the mean velocity vector, ρ – the fluid's density, k – the kinetic energy of turbulence, and $\mu_{\text{ef}} = \mu + \mu_t$ – the effective viscosity, where μ is molecular viscosity and μ_t – turbulent viscosity.

The Reynolds system of equations is closed by equations of the turbulence model [5, 6]. At present, the so-called viscosity turbulence models are widely used. They are based on the idea of turbulent viscosity considered as a scalar quantity. These models include algebraic models (without equations) and models containing one or more equations (usually two). Taking into account the employed constitutive relations, we may distinguish the following viscosity models:

- linear models – based on the classical Boussinesq hypothesis, postulating a linear relation between the Reynolds stress tensor and the tensor of deformation rate, or
- non-linear models – based on generalizations of the Boussinesq hypothesis, where this relation is non-linear.

The Launder-Spalding k-ε model [7] of 1974, including two equations, is the most widely used linear model. There are many other linear and non-linear models. In this paper, the authors have used the above-mentioned Launder-Spalding model, the RNG k-ε model proposed by Yakhot *et al.* [8], the realizable k-ε model formulated by Shih *et al.* [9] and two variants of the k-ω model [5].

In the standard Launder-Spalding k-ε model, turbulent viscosity is calculated from the following equation:

$$\mu_{\text{ef}} = \rho c_\mu \frac{k^2}{\varepsilon}. \tag{3}$$

Distributions of kinetic energy of turbulence, k, and the dissipation rate of kinetic energy of turbulence, ε, are obtained from the following equations:

$$\rho\nabla\cdot k\mathbf{U} = \nabla\cdot\left(\mu + \frac{\mu_t}{\sigma_k}\right)\nabla k + G - \rho\varepsilon, \tag{4}$$

$$\rho\nabla\cdot\varepsilon\mathbf{U} = \nabla\cdot\left(\mu + \frac{\mu_t}{\sigma_\varepsilon}\right)\nabla\varepsilon + \frac{\varepsilon}{k}(c_1 G - c_2\rho\varepsilon). \tag{5}$$

The exact value of the production of turbulence kinetic energy term, G, is determined from as follows:

$$G = -\rho\overline{u_i' u_j'}\frac{\partial U_j}{\partial x_i}. \tag{6}$$

Taking into account the Boussinesq hypothesis postulating a linear relation between the Reynolds stress tensor and the tensor of deformation rate, we can approximate $\rho\overline{u_i' u_j'}$ from Equation (6) by:

$$-\rho\overline{u_i' u_j'} = \mu_t \left(\frac{\partial U_i}{\partial x_j} + \frac{\partial U_j}{\partial x_i} \right) - \frac{2}{3}\rho k \delta_{ij}. \tag{7}$$

The turbulence model described by Equations (3)–(7) includes a set of numerical coefficients, σ_k, σ_ε, c_1, c_2, c_μ, which are usually called "constants". These coefficients are determined in experiments. The values recommended by Launder and Spalding are:

$$\sigma_k = 1.00, \quad \sigma_\varepsilon = 1.30, \quad c_1 = 1.44, \quad c_2 = 1.92, \quad \mu = 0.09, \tag{8}$$

although their modifications have been proposed in some papers [10].

Equations of the RNG k-ε model have been derived with use of so-called Renormalization Group Theory [11]. However, they are similar to the equations of the traditional k-ε model. The equation for k is the same as in the Launder-Spalding model, while the equation for ε contains an additional component:

$$-\frac{c_\mu \eta^3 (1 - \eta/\eta_0)}{1 + \beta\eta^3} \frac{\varepsilon^2}{k}, \tag{9}$$

where

$$\eta = \sqrt{\frac{G}{c_\mu \rho \varepsilon}}. \tag{10}$$

The model coefficients' values are as follows:

$$\sigma_k = 0.8, \ \sigma_\varepsilon = 1.15, \ c_1 = 1.42, \ c_2 = 1.68, \ c_\mu = 0.0865, \ \eta_0 = 4.38, \ \beta = 0.012. \tag{11}$$

The value of the c_μ coefficient has been obtained from theoretical considerations, but it is close to the value determined in experiments, *i.e.* 0.09.

In addition to the standard and RNG-based k-ε models, we can also provide the so-called realizable k-ε model [9]. The term "realizable" means that the model satisfies certain mathematical constraints on normal stresses, consistent with the physics of turbulent flows. This model was intended to address these deficiencies of the traditional k-ε models by adopting the following:

(a) a new eddy-viscosity formula involving a c_μ variable and
(b) a new model equation for dissipation based on the dynamic equation of the mean-square vorticity fluctuation.

Variable c_μ is computed from:

$$c_\mu = \frac{1}{A_0 + A_S \frac{kU^*}{\varepsilon}}, \tag{12}$$

$$U^* = \sqrt{S_{ij} S_{ij} + \widetilde{\Omega}_{ij} \widetilde{\Omega}_{ij}}, \tag{13}$$

$$\widetilde{\Omega}_{ij} = \overline{\Omega}_{ij} - 3\,\varepsilon_{ijk}\,\omega_k, \tag{14}$$

where $\overline{\Omega}_{ij}$ is the mean rate-of-rotation tensor viewed in a rotating reference frame of angular velocity ω_k. Model constants A_0 and A_S are given by:

$$A_0 = 4.04, \quad A_S = \sqrt{6}\cos\phi, \tag{15}$$

where

$$\phi = \frac{1}{3}\cos^{-1}\left(\sqrt{6}W\right),\ W = \frac{S_{ij}S_{jk}S_{ki}}{\widetilde{S}},\ \widetilde{S} = \sqrt{S_{ij}S_{ij}},\ S_{ij} = \frac{1}{2}\left(\frac{\partial U_i}{\partial x_j} + \frac{\partial U_j}{\partial x_i}\right). \quad (16)$$

The modeled transport equation for ε is as follows:

$$\rho\nabla\cdot\varepsilon\mathbf{U} = \nabla\cdot\left(\mu + \frac{\mu_t}{\sigma_\varepsilon}\right)\nabla\varepsilon - \rho\, c_2 \frac{\varepsilon^2}{k + \sqrt{\frac{\mu}{\rho}}\varepsilon}. \quad (17)$$

Model constants c_2, σ_k, and σ_ε have been established to ensure that the model performs well for certain canonical flows:

$$\sigma_k = 1.0, \quad \sigma_\varepsilon = 1.2, \quad c_2 = 1.9. \quad (18)$$

Another approach to turbulence modeling is exemplified by the standard and shear-stress transport (SST) k-ω models [5]. The models are similar in form, with transport equations for k and ω. The major differences between the SST model and the standard model are as follows:

(a) gradual change from the standard k-ω model in the inner region of the boundary layer to a high-Reynolds-number version of the k-ε model in the outer part of the boundary layer, and
(b) modified turbulent viscosity formulation to account for the transport effects of the principal turbulent shear stress.

The standard k-ω model is an empirical model based on model transport equations for the turbulence kinetic energy, k, and the specific dissipation rate, ω, which can also be thought of as the ε to k ratio:

$$\rho\nabla\cdot k\mathbf{U} = \nabla\cdot\left(\mu + \frac{\mu_t}{\sigma_k}\right)\nabla k + G - Y_k, \quad (19)$$

$$\rho\nabla\cdot\varepsilon\mathbf{U} = \nabla\cdot\left(\mu + \frac{\mu_t}{\sigma_\omega}\right)\nabla\varepsilon + \frac{\omega}{k}G - Y_\omega, \quad (20)$$

where Y_k and Y_ω represent the dissipation of k and ω due to turbulence.

Turbulent viscosity, μ_t, is computed by combining k and ω as follows:

$$\mu_t = \rho\frac{k}{\omega}. \quad (21)$$

Dissipation of k is given by:

$$Y_k = \rho\beta^* f_{\beta^*} k\omega, \quad (22)$$

where

$$f_{\beta^*} = \begin{cases} 1 & \text{for } \chi_k^2 \le 0, \\ \dfrac{1+680\chi_k^2}{1+400\chi_k^2} & \text{for } \chi_k^2 > 0, \end{cases} \quad (23)$$

wherein

$$\chi_k \equiv \frac{1}{\omega^3}\frac{\partial k}{\partial x_j}\frac{\partial \omega}{\partial x_j}. \quad (24)$$

Dissipation of ω is given by:

$$Y_\omega = \rho\beta f_\beta \omega^2, \quad (25)$$

where

$$f_\beta = \frac{1+70\chi_\omega}{1+80\chi_\omega}, \quad (26)$$

wherein

$$\chi_\omega = \left| \frac{\Omega_{ij}\Omega_{jk}S_{ki}}{(\beta^*\omega)^3} \right|, \tag{27}$$

$$\Omega_{ij} = \frac{1}{2}\left(\frac{\partial U_i}{\partial x_j} - \frac{\partial U_j}{\partial x_i} \right). \tag{28}$$

Model constants are as follows:

$$\sigma_k = 2.0, \quad \sigma_\varepsilon = 2.0, \quad \beta^* = 0.09, \quad \beta = 0.072. \tag{29}$$

The variation of the k-ω model is called the shear-stress transport (SST) k-ω model, so named because the definition of turbulent viscosity is modified to account for the transport of principal turbulent shear stress. Other modifications include the addition of a cross-diffusion term in the ω equation and a blending function to ensure that the model equations behave appropriately both in the near-wall and the far-field zones:

$$\rho\nabla\cdot\varepsilon\mathbf{U} = \nabla\cdot\left(\mu + \frac{\mu_t}{\sigma_\omega}\right)\nabla\varepsilon + \frac{\omega}{k}G - Y_\omega + D_\omega. \tag{30}$$

Turbulent viscosity, μ_t, is computed as follows:

$$\mu_t = \rho\frac{k}{\omega}\frac{1}{\max\left[1, \dfrac{\Omega F_2}{a_1\omega}\right]}, \tag{31}$$

where

$$\Omega = \sqrt{2\Omega_{ij}\Omega_{ij}}, \tag{32}$$

$$\sigma_k = \frac{1}{F_1/\sigma_{k,1} + (1-F_1)/\sigma_{k,2}}, \tag{33}$$

$$\sigma_\omega = \frac{1}{F_1/\sigma_{\omega,1} + (1-F_1)/\sigma_{\omega,2}}. \tag{34}$$

$\Omega_{ij}$is the mean rate-of-rotation tensor. The blending functions, F_1 and F_2, are given by:

$$F_1 = \tanh\left(\Phi_1^4\right), \tag{35}$$

$$\Phi_1 = \min\left[\max\left(\frac{\sqrt{k}}{0.09\omega y}, \frac{500\mu}{\rho y^2\omega}\right), \frac{4\rho k}{\sigma_{\omega,2}D_\omega^+ y^2}\right], \tag{36}$$

$$D_\omega^+ = \max\left[2\rho\frac{1}{\sigma_{\omega,2}}\frac{1}{\omega}\frac{\partial k}{\partial x_j}\frac{\partial\omega}{\partial x_j}, 10^{-20}\right], \tag{37}$$

$$F_2 = \tanh\left(\Phi_2^2\right), \tag{38}$$

$$\Phi_2 = \max\left[2\frac{\sqrt{k}}{0.09\omega y}, \frac{500\mu}{\rho y^2 \omega}\right], \tag{39}$$

where y is the distance to the next surface and D_ω^+ is the positive portion of the cross-diffusion term. D_ω is defined as:

$$D_\omega = 2(1-F_1)\rho\sigma_{\omega,2}\frac{1}{\omega}\frac{\partial k}{\partial x_j}\frac{\partial \omega}{\partial x_j}. \tag{40}$$

Additional model constants are as follows:

$$\sigma_{k,1} = 1.176, \quad \sigma_{\omega,1} = 2.0, \quad \sigma_{k,2} = 1.0, \quad \sigma_{\omega,2} = 1.168, \quad a_1 = 0.31. \tag{41}$$

3. Area of calculations, boundary conditions and discretization

The FLUENT computer program, made by Fluent Inc. [12], was used to simulate the flow. The equations of particular turbulence models, together with the set of equations of motion completed with the equation of continuity, are solved with the finite element method. The area of calculations includes a straight section of the pipeline with the measuring orifice (Figure 1).

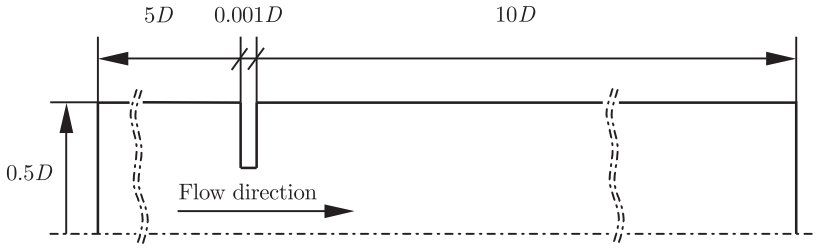

Figure 1. Area of calculations

The area of calculations is discretized with use of a two-dimensional rectangular grid, refined near the orifice (Figure 2).

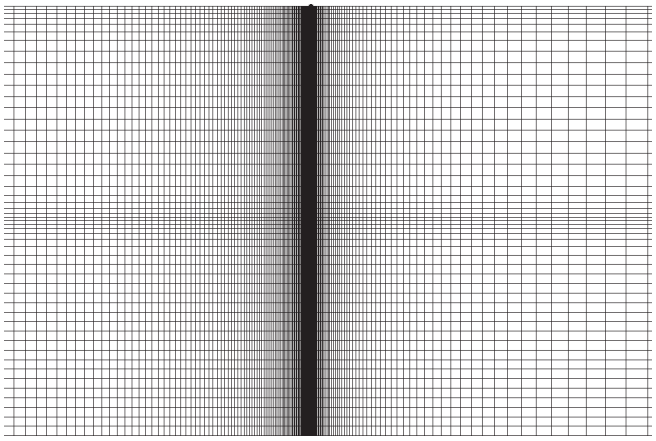

Figure 2. Arrangement of the grid nodes near the orifice

Calculations were performed for many different grid sizes. The following boundary conditions are assigned in FLUENT:

- Inlet – the boundary conditions in the inlet section were given with use of data obtained from calculations of 60D straight pipe flow,
- Outlet – the pressure outlet,
- Center-line – the axis,
- Pipe wall – the wall (standard wall function).

The test of convergence was calculated from:

$$\left\| \frac{\phi_n - \phi_{n-1}}{\phi_n} \right\| \leq \delta_{tol}, \tag{42}$$

where ϕ_n is the vector of unknowns and n denotes an iteration step, calculated separately for each degree of freedom, $\|\bullet\|$ – root mean square norm, $\delta_{tol} = 0.0001$.

4. Results of numerical calculations

The calculation results were compared with the experimental data obtained by Morrison *et al.* [13] with the use of a laser anemometer. The size of the differential grid is one of the most important parameters influencing the accuracy of the obtained results. The influence of the number of nodes of the differential grid on velocity at the pipeline symmetry axis is shown in Figure 3.

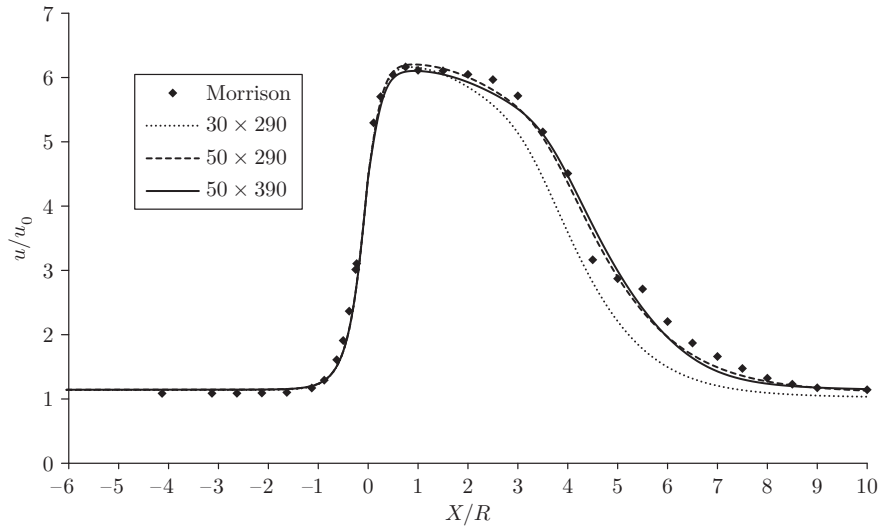

Figure 3. Normalized velocity at the axis for various grid sizes

Apparently, increased number of nodes leads to better conformity of the results of simulation and experiments. A similar rule applies when kinetic energies of turbulence are compared (see Figure 4), although the influence of the number of nodes on the accuracy of results is not so apparent. The increase in the number of nodes from 50×290 to 50×390 does not strongly influence the obtained results, so a 50×290 grid was chosen for comparison of turbulence models.

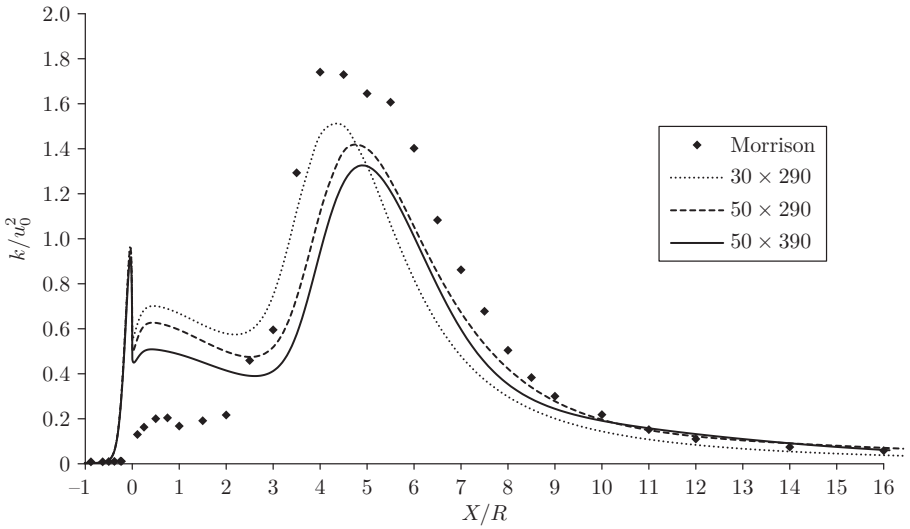

Figure 4. Normalized kinetic energy of turbulence at the axis for various grid sizes

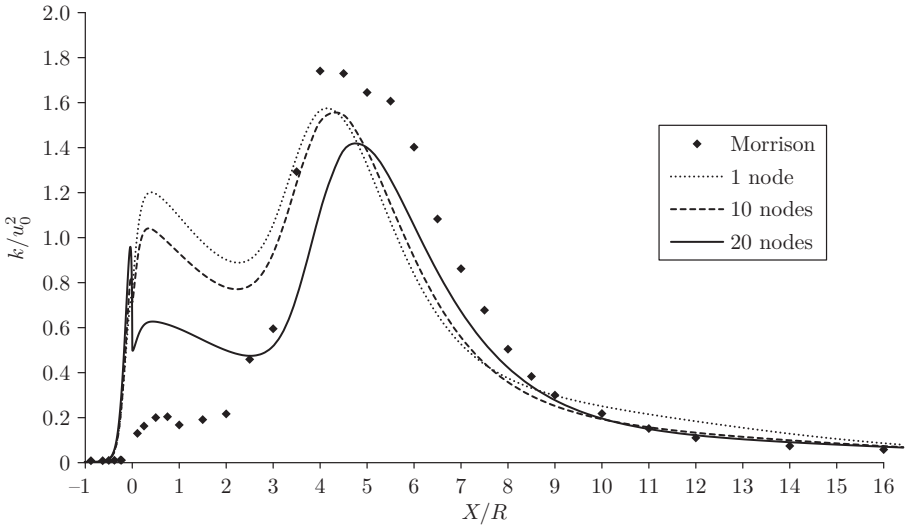

Figure 5. Normalized kinetic energy of turbulence at the axis for various grid sizes within the orifice

Calculations the results of which are shown in Figures 3–5 were performed with the use of the Launder-Spalding standard k-ε model, but a similar tendency can be observed in the case of other turbulence models.

In Figure 6 comparisons of velocity distributions in the pipeline axis are shown for five different turbulence models and a 50×290 grid. The Launder-Spalding model is evidently superior to the other models, and velocity changes are well represented qualitatively.

Figure 7 offers a comparison of turbulence kinetic energy distributions at the pipeline axis for five different turbulence models and a 50×290 grid. Although a large scatter of calculation results can be observed and all of the calculated results differ

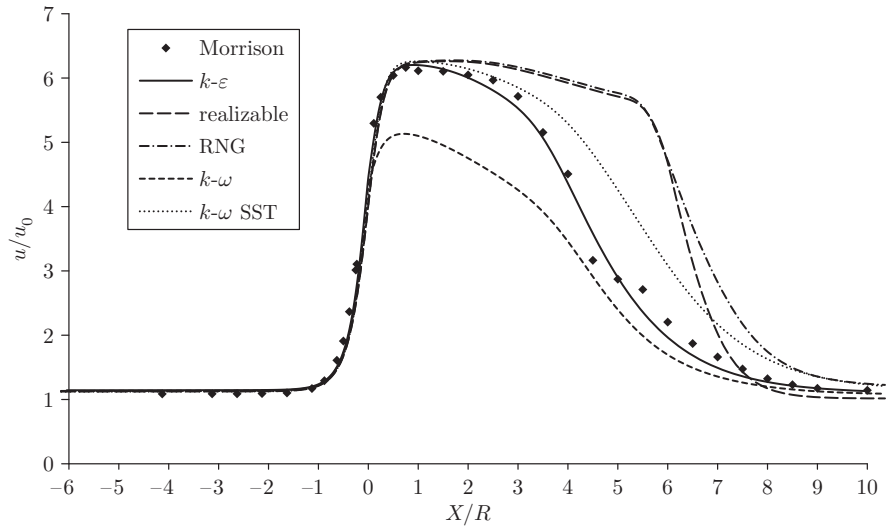

Figure 6. Normalized velocity at the axis for various turbulence models, 50×290 grid

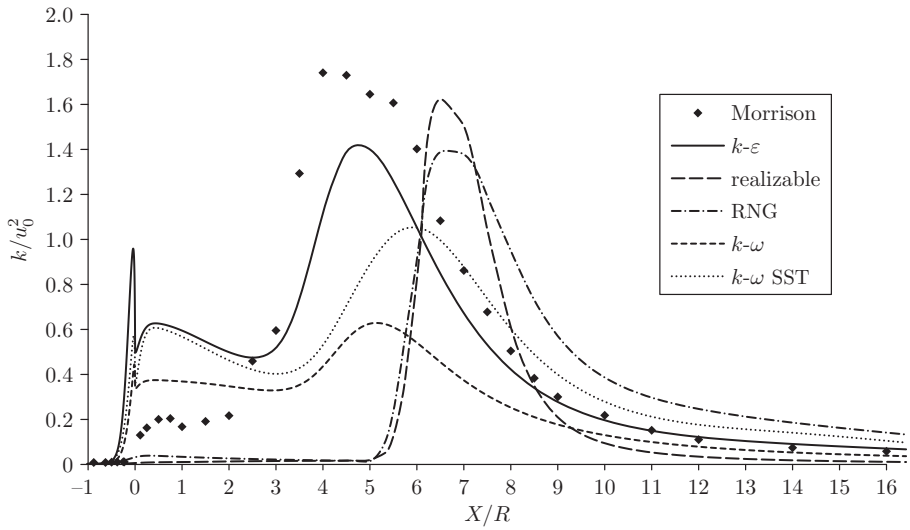

Figure 7. Normalized kinetic energy of turbulence at the axis for various turbulence models, 50×290 grid

from the experimental results, the values obtained from the Launder-Spalding model are the closest to the results obtained from experiment.

5. Conclusions

Numerical simulation of a two-dimensional flow through a pipeline with an orifice has been performed with use of a modern CFD program. It appears from a comparison of the obtained data with experimental data that the assumed turbulence model strongly influences the obtained results.

The best conformity with measurement results was obtained for a differential grid of 50×290 nodes (increase in the number of nodes to 50×390 does not

significantly improve the results) and for the Launder-Spalding k-ε turbulence model. None of the tested turbulence models reflects the real distribution of the kinetic energy of turbulence at the symmetry axis. It appears from the performed simulations that when simulating a two-dimensional flow, the traditional Launder-Spalding model yields the best results and involves the lowest calculation cost.

References

[1] Burden T L and McLaury B S 2002 *Experiments in Fluids* **32** 472
[2] Erdal A and Andersson H I 1997 *Flow Meas. Instr.* **8** (1) 27
[3] Hilgenstock A and Ernst R 1996 *Flow Meas. Instr.* **7** 161
[4] Spencer E A, Heitor M V and Castro I P 1995 *Flow Meas. Instr.* **6** (1) 3
[5] Wilcox D C 1998 *Turbulence Modeling for CFD*, DCW Industries, Inc., La Canada, California
[6] Pope S B 2000 *Turbulent Flows*, Cambridge University Press
[7] Launder B E and Spalding D B 1974 *Comp. Meth. Appl. Mech. Eng.* **3** 269
[8] Yakhot V, Orszag S A, Thangam S, Gatski T B and Speziale C G 1992 *Physics of Fluids* **A4** (7) 1510
[9] Shih T-H, Liou W W, Shabbir A, Yang Z and Zhu J 1995 *Computers Fluids* **24** (3) 227
[10] Reader-Harris M J 1986 *Proc. Int. Conf. on Flow Measurement in the Mid 80's*, National Engineering Laboratory, East Kilbridge, Glasgow, Paper 7.3
[11] Yakhot V and Orszag S A 1986 *J. Sci. Comp.* **1** 1
[12] *Fluent. Fluid Dynamics Analysis Package*, Fluid Dynamics International, Inc., 2005
[13] Morrison G L, DeOtte R E (jr), Nail G H and Panak D L 1993 *AIChE J.* **39** (5) 745